RAPID COMMUNICATIONS

PHYSICAL REVIEW E VOLUME 53, NUMBER 3 MARCH 1996

Subpicosecond compression of 0.1–1 nC electron bunches with a magnetic chicane at 8 MeV

Bruce E. Carlsten and Steven J. Russell
Los Alamos National Laboratory, Los Alamos, New Mexico 87545
(Received 22 September 1995)

After compressing electron bunches with a half-meter long, four-dipole chicane at 8 MeV, we have measured full width at half maximum (FWHM) bunch lengths of less than 1 ps for charges from 0.1 to 1.1 nC. The uncompressed FWHM bunch lengths varied from 10 to 20 ps, and we achieved compression ratios in excess of 40 and peak currents greater than 1 kA. Bunch lengths for low charges were measured using a transversely deflecting rf cavity; bunch lengths for high charges were inferred from the energy spread induced in the beam by its longitudinal space-charge force as it drifted from the end of the compressor to the spectrometer.

PACS number(s): 29.27.Bd, 41.75.Ht

We have constructed an 8-MeV accelerator capable of subpicosecond compression of electron bunches with charges up to 3 nC [1]. This linac will be used both for fundamental bunch compression research and to drive an extreme ultraviolet source, using the anomalous energy loss of a short electron bunch in a plasma due to the induced wakefield [2]. This type of source is considered as an option for next-generation lithography [3]. The accelerator is based on an 8-MeV photoinjector, previously used for free-electron laser experiments [4], and incorporates a four-dipole chicane for the bunch compression. This injector was used for the proof-of-principle experiments demonstrating the space-charge induced emittance compensation scheme [4–6], and is capable of producing very low emittance electron bunches. Typical normalized rms emittances from this injector are 2.5 π mm mrad per nC of charge in the bunch, which is significantly lower than emittances attainable for beams from thermionic cathodes. The chicane was carefully designed to allow both first- and second-order matching of the electron bunch's energy-phase correlation, making this accelerator designed specifically for maximizing compression. As a result, this accelerator is capable of subpicosecond compression of larger bunch charges than that reported in other experiments [7,8], by over an order of magnitude. The novel use of a photoelectric injector allows tailoring of the bunch's initial longitudinal phase space, which allows maximum flexibility in establishing the desired bunch energy-phase correlation and ensures that the bunch's tails are compressed tightly as well as the center of the bunch.

The low beam emittance and high bunch charge facilitates the use of this accelerator to study space-charge induced emittance-growth mechanisms of compressor systems that would not be apparent in higher-emittance beams [9]. This is important for many advanced accelerator applications (linear colliders, short-wavelength free-electron lasers, and plasma accelerators, among others) that require subpicosecond compression of at least 1 nC with very low compressed emittances, on the order of 1 π mm mrad per nC of charge, or less. In addition, there are many solid-state and atomic-physics applications that are enabled by extremely short, high-brightness electron bunches.

Prompt electron emission from a cathode on the upstream end of the 5.5-cell, standing-wave, 1.3-GHz photoinjector is triggered by an ultraviolet drive laser pulse of variable radius, length, and timing relative to the rf in the tank. The drive laser is typically timed such that the electrons are emitted very early in the rf cycle, well before the field in the first cell is peaked. This ensures that the electrons at the rear of the bunch have a higher energy after they exit the tank than those at the front. After the electrons leave the accelerator they encounter an independently phased rf cavity, called the phasing cavity. The purpose of this cavity is to add additional control over the beam's energy-phase distribution. In general, this cavity is phased such that the center of the bunch does not change energy, the front of the bunch is decelerated, and the rear is accelerated. The four-dipole chicane compressor fits in the beamline after the phasing cavity and consists of four uniform-field, parallel-faced dipoles, shown schematically in Fig. 1. There is no drift between the dipoles, and each dipole is about 9.25 cm wide. The dipole pole faces have an H-magnet geometry, which minimizes the fringing fields. The first and last dipole deflect the beam upwards and the middle two dipoles deflect the beam downwards. Particles with higher energy are bent less and have a shorter path length within the dipoles than particles with lower energy. By adjusting the energy slew along the bunch by changing the phasing cavity gradient and drive laser phase, the bunch can be compressed and the particles initially at both the front and the rear of the bunch leave the chicane at essentially the same time. The beam box is large enough to allow transport of deflection angles θ of up to 45°. The beamline is discussed in detail in Ref. [1].

Initial experiments were carried out at low charge (about

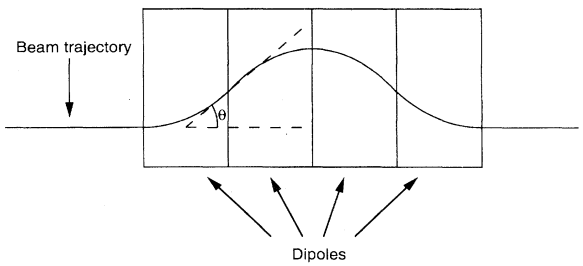

FIG. 1. Schematic of a four-dipole chicane compressor, showing chicane bend angle θ. Low energy particles have a longer path length than high energy particles.

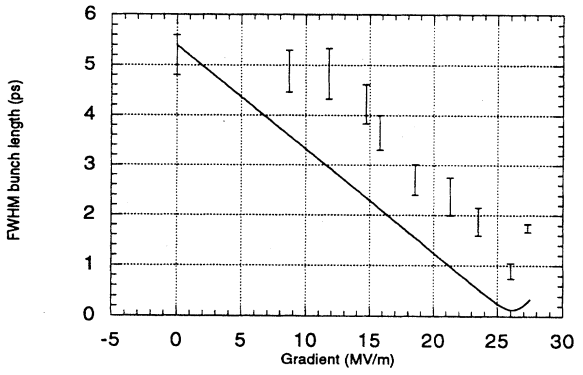

FIG. 2. Compressed FWHM bunch length versus phasing cavity gradient (with error bars), compared to PARMELA simulations (solid line), for 0.1 nC.

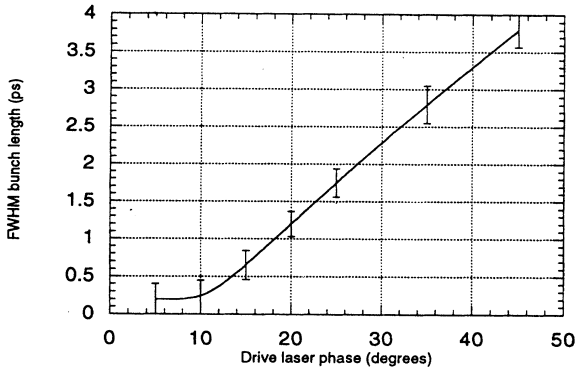

FIG. 3. Compressed FWHM bunch length versus drive laser phase (with error bars), compared to theoretical fit (solid line), for 0.1 nC.

0.1 nC). The chicane deflection angle was set to about 40°, and then either the phase of the drive laser relative to the rf was varied or, more commonly, the field strength in the phasing cavity was changed while it was phased for no energy gain of the bunch center. The compressed bunch length at low charge was measured by using a transversely deflecting rf cavity, operating in the TM_{110} mode. This cavity, known as the fast deflector, imparts a transverse velocity on the particles correlated with their relative axial position in the bunch. The amount of relative deflection between the front and rear of the bunch can be found by intercepting the beam by a diagnostic screen. The deflection was calibrated by monitoring how much the spot shifted on the screen as the phase of the fast deflector was changed slightly, and for typical focusings the deflection varied from 0.035 ps/pixel to 0.065 ps/pixel. With the fast deflector off, the minimum full width at half maximum (FWHM) spot size was typically 10 pixels, which varied less than 10% over the different drive laser phases and phasing cavity gradients used. With the fast deflector on, the FWHM bunch length was found by subtracting the resolution limit (10 pixels) from the streaked spot size in quadrature. In Fig. 2 we plot the deconvolved measured FWHM bunch length as a function of gradient in the phasing cavity, as well as bunch length predictions by the accelerator simulation code PARMELA [10]. For the cases shown, the drive laser FWHM pulse length was 20 ps (both measurements and simulations indicate that the FWHM electron bunch length was about 10 ps at the exit of the accelerator due to rf compression in the photoinjector). In Fig. 3 we see the deconvolved measured FWHM bunch length as a function of drive laser phase relative to the rf in the accelerator tank, for a fixed gradient in the phasing cavity (26 MV/m). At the phase leading to the minimum bunch length, both the initial energy slew and curvature are matched by the dispersion in the chicane. As the drive laser phase is increased, the mismatch in both the slew and curvature leads to a larger compressed bunch length, which is easily predicted. (The photoinjector contributes no slew at a phase of 60°; since the photoinjector and phasing cavity can add in approximately the same amount of slew, the compressed bunch length at 60° with the phasing cavity on should be about the same as the compressed bunch length with the drive laser phased for maximum slew but with the phasing cavity off, shown in Fig. 2, which it is.) The solid line in Fig. 3 is a numerical fit in which the bunch length is found from adding in quadrature the minimum bunch length and the effect from the changes in the energy-phase correlation for different drive laser phases. The minimum deconvolved measured bunch length was less than the net resolution of this measurement, about 0.25 ps. The compression ratio for this case was at least 40.

At higher charges (near 1 nC), the increased emittance of the beam degraded the fast deflector resolution. For this case we used the induced energy spread on the beam as it drifts after compression to infer the peak current of the bunch.

If the beam is sufficiently relativistic so that its length is large compared to its radius in its own frame of reference, the axial electric field for a beam with a uniform radial profile as it drifts is given by [9]

$$E_z=\frac{\partial I}{\partial\zeta}\frac{1}{2\pi\varepsilon\beta\gamma^2 c a^2}\left(\frac{a^2-r^2}{2}+a^2\ln\frac{b}{a}\right) \tag{1}$$

where the beam current I is a function of both axial position away from the chicane and relative axial position ζ within the bunch, a is the beam radius and b is the beam pipe radius. If the radial profile is not uniform there are some changes to the form of the field, but in all cases it depends linearly on $\partial I/\partial\zeta$, which scales as I_{peak}^2/Q where Q is the bunch charge or Q/τ^2, where τ is the bunch length. Thus the energy spread induced as the beam drifts can be expected to be

$$\frac{\Delta\gamma}{\gamma}=c_1\frac{I^2}{Q\gamma^3}=c_2\frac{Q}{\tau^2\gamma^3} \tag{2}$$

where c_1 and c_2 are some constants. The induced energy spread subtracts from the initial energy spread if the beam is undercompressed in the chicane, and adds to the initial energy spread if the beam is overcompressed, because in both cases there is still a well-correlated energy-phase relationship after the chicane. However, for the case of maximum compression, this original correlation vanishes, and the final energy spread is given by the induced energy spread added in quadrature with the original energy spread. Thus, we predict that the measured energy spread at the spectrometer de-

creases a little and then increases quickly as the chicane bend angle is increased from zero to the angle of maximum compression.

In order to eliminate ambiguity while using the induced energy spread to infer the peak current, we kept the initial energy slew along the bunch constant and only varied the magnetic field in the chicane dipoles to change the level of compression. This is done because the magnetic field itself cannot modify the energy distribution of the particles—any change in the energy spread of the particles as they reach the spectrometer has to arise from changes in their space-charge fields, as indicated in Eq. (2). This fact is essential in arguing that any observed increase in the energy spread is induced just by the increased longitudinal space-charge force after compression.

To use this technique to infer the bunch length, we also need a high level of confidence in the ability of our simulation tool PARMELA to establish a relation between the compressed bunch length and the measured induced energy spread, which we will then use to infer the compressed bunch length from induced energy spread measurements. We have benchmarked the longitudinal space-charge force calculation in this version of PARMELA by comparing the simulated bunch length expansion (or contraction) of different electron bunches in this photoelectric injector with streak-camera measurements [4,11]. This comparison is relevant because both the induced energy spread after compression and the bunch length expansion (contraction) in the photoinjector are dominated by the $\partial I/\partial\zeta$ term in Eq. (1). These comparisons were made for bunch charges varying from 1–5 nC and for several different phases of the drive laser relative to the rf, all with drive laser FWHM pulse lengths of 10 ps. During acceleration in the photoinjector, the longitudinal space-charge force tries to expand the bunch length whereas the rf acceleration process itself tends to compress the bunch length (because the tail of the bunch experiences a larger accelerating rf field than the front), and these two effects cancel to a large fraction. There was less than a 10% error between the prediction (using PARMELA) and streak camera measurement of both the amount of contraction of a 1 nC bunch (from 10 to 7 ps) and the amount of expansion of a 5 nC bunch (from 10 to 15 ps). Because the rf forces (which are well known) and the space-charge forces (which we want to find) cancel to at least 50% for the cases compared, this agreement indicates that the error in the longitudinal space charge force is somewhat less than 5%. This error is negligible in comparison to our experimental uncertainty in bunch charge (about 30%). Using Eq. (2), we estimate that the total error in this procedure of measuring the compressed bunch length is about 30% (using a 30% uncertainty in the charge, an additional equivalent 10% charge uncertainty from different possible beam envelopes between the chicane and spectrometer, and 5% uncertainties in the beam energy and energy spread measurements).

The $\partial I/\partial\zeta$ term in Eq. (1) can be thought of introducing a linear energy slew along the bunch, with some small higher-order distortion. The linear part dominates both the induced energy spread and the bunch length expansion. However, the minimum compressed bunch length is heavily influenced by the higher-order features in the energy-phase correlation before the chicane (because to lowest order the chicane bending angle is adjusted to remove the linear part of the initial energy slew). These higher-order features (quadratic and cubic curvature, as well as the instantaneous energy spread for a given thin axial slice within the bunch) are complicated functions of the wake potentials, beam radius, and other parameters within the accelerator, and are hard to predict with simulations. Thus, we can use these benchmarked simulations to predict the compressed bunch length from the measured induced energy spread, but not necessarily to predict the compressed bunch length from the accelerator setup to the same accuracy.

In Fig. 4 we show a FWHM energy spread measurement as the chicane angle is changed for a typical 0.67 nC case, where the unbunched energy spread is about 2.5% at the spectrometer (and about 3.5% at the entrance to the chicane). Note both the prominent energy spread decrease and the subsequent peak as the chicane bend angle is increased, as expected. The error bars shown indicate the accuracy of each measurement, averaged over several individual measurements, and do not include any systematic errors. The accelerator setup was carefully modeled in PARMELA. The actual drive laser pulse had a FWHM of 20 ps, but fairly long tails. Because of streak camera resolution issues, the amount of charge in the tails was determined by measuring the beam's energy distribution in the spectrometer, with both the phasing cavity and chicane turned off. The deconvolved charge distribution was represented in the simulations by superimpos-

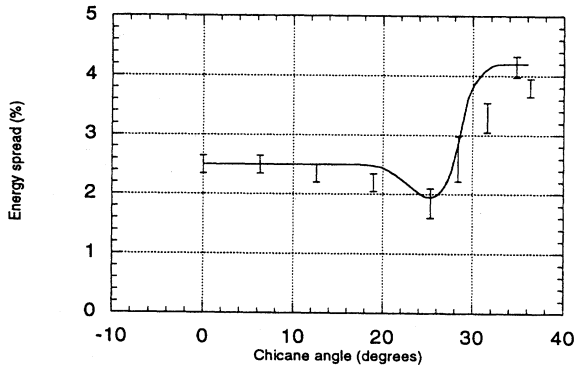

FIG. 4. Measured energy spread in the spectrometer versus chicane bending angle (with error bars), compared to PARMELA simulations (solid line), for 0.67 nC.

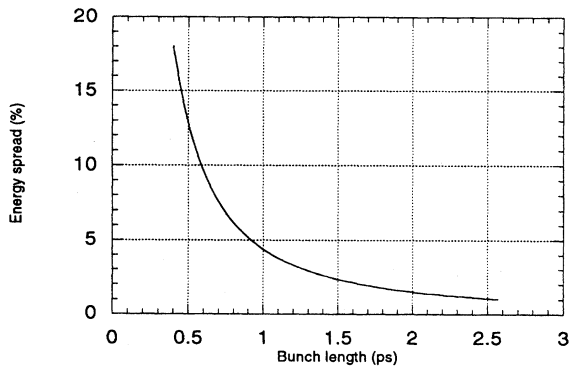

FIG. 5. PARMELA simulation results of induced energy spread versus FWHM bunch length for a 1.1 nC bunch.

ing two Gaussian distributions with different rms widths for the initial electron distribution. The simulations results for this case are included in Fig. 4, and the agreement is quite good. The minimum FWHM bunch length in the PARMELA simulations is about 0.4 ps, with a peak current of about 1.1 kA, which is thereby inferred to be the minimum bunch length and maximum current during compression for this case.

We have also measured induced energy spreads of 9.0% for a bunch charge of 1.1 nC at a chicane bend angle of 29°. In Fig. 5 we plot the induced energy spread versus compressed bunch length, for a series of 1.1 nC PARMELA simulations, using the spectrometer measurements to reconstruct the initial beam distribution. Note in Fig. 5 that the induced energy spread scales very closely to the inverse square of the compressed bunch length, in agreement with Eq. (2). The peak induced energy spread found in the simulations (16%) was not seen in the experiment, implying that the bunch length never reached 0.4 ps. This might be due to an unaccounted excessive instantaneous energy spread (at a given axial slice of the bunch), or distortions in the energy-phase correlation before the chicane perhaps resulting from additional wakefields not included in the simulation. However, because the peak induced energy spread is directly correlated to the minimum bunch length, we can use Fig. 5 to infer the minimum bunch length in the experiment—for an induced energy spread of 9.0%, this implies a minimum FWHM bunch length of about 0.7 ps (and a peak current of 1.4 kA).

This work was supported by the Los Alamos Laboratory Directed Research and Development program and by a Los Alamos CRADA with Northrop-Grumman, CRADA No. LA93C10102, under the auspices of the U.S. Department of Energy. We are pleased to acknowledge the contributions of J. Kinross-Wright, D. Feldman, M. Weber, J. Plato, M. Milder, R. Cooper and R. Sturges during the construction and operation of the accelerator.

[1] B. E. Carlsten *et al.* (unpublished).
[2] R. Keinigs, M. E. Jones, and J. J. Su, IEEE Trans. Plasma Sci. **PS-15**, 199 (1987).
[3] R. D. Fulton *et al.* (unpublished).
[4] P. G. O'Shea *et al.*, Nucl. Instrum. Phys. Res. A **331**, 62 (1993).
[5] B. E. Carlsten, Part. Accel. **49**, 27 (1995).
[6] J. C. Gallardo and H. G. Kirk, *Proceedings of the 1993 Particle Accelerator Conference*, IEEE catalog No. 93CH3279-7, 3615 (IEEE, New York, 1993).
[7] M. Uesaka, K. Tauchi, T. Kozawa, T. Kobayashi, U. Ueda, and K. Miya, Phys. Rev. E **50**, 3068 (1994).
[8] P. Kung, H. Lihn, and H. Wiedemann, Phys. Rev. Lett. **73**, 967 (1994).
[9] B. E. Carlsten and T. O. Raubenheimer, Phys. Rev. E **51**, 1453 (1995).
[10] L. Young (private communication).
[11] A. H. Lumpkin, B. E. Carlsten, and R. B. Feldman, Nucl. Instrum. Phys. Res. A **304**, 374 (1991).